

## **GAIN BANDWIDTH OF PHONON-COOLED HEB MIXER MADE OF NBN THIN FILM WITH MgO BUFFER LAYER ON Si.**

Yuriy B. Vachtomin, Matvey I. Finkel, Sergey V. Antipov, Boris M. Voronov, Konstantin V. Smirnov, Natalia S. Kaurova, Vladimir N. Drakinski and Gregory N. Gol'tsman

*Physics Department, Moscow State Pedagogical University, Moscow 119435, Russia.*

### **Abstract.**

We present recently obtained values for gain bandwidth of NbN HEB mixers for different substrates and film thicknesses and for MgO buffer layer on Si at LO frequency of 0.85–1 THz. The maximal bandwidth, 5.2 GHz, was achieved for the device on MgO buffer layer on Si with a 2 nm thick NbN film. Functional devices based on NbN films of such thickness were fabricated for the first time due to an improvement of superconducting properties of NbN film deposited on MgO buffer layer on Si substrate.

### **Introduction.**

In the last years, the development of HEB mixers has reached such a high level that these devices can be successfully utilized in heterodyne receivers of THz frequency range. Their high sensitivity and low LO power make them suitable for radioastronomic observations on space- and airborne platforms. An NbN HEB mixer seems to be a preferable mixing device now for such projects as FIRST (Far Infrared Receiver Satellite Telescope), GREAT (German REceiver for Astronomy Terahertz frequencies), or TELIS (TErahertz Limb Sounder). Heterodyne receiver based on this type of mixer is successfully used on the 10-m Heinrich Hertz Telescope on Mount Graham, Arizona [1]. The obtained values of noise temperature for a receiver based on NbN HEB mixer are 650 K at LO frequency of 1.6 THz and 1100K at 2.5 THz [2]. These noise characteristics amount to 5-10 times of the quantum limit.

Currently phonon- [3] and diffusion- cooled [4] HEB mixers are being developed. The main difference between the two modifications lies in the electron cooling mechanism. In the diffusion cooled HEB mixer, the electron subsystem is relaxed by the diffusion of nonequilibrium hot electrons to cold metal contact pads. The gain bandwidth in this case is

determined by the length of the active superconducting film and the electron diffusion coefficient and reaches 9 GHz for 80 nm long Nb microbridge [5].

In the case of the phonon-cooled HEB mixer, electron temperature is relaxed by electron-phonon interaction and later by the escape of non-equilibrium phonons to the substrate [6]. Gain bandwidth of this type of HEB mixer depends on electron-phonon interaction time  $\tau_{\text{eph}}$  and on the non-equilibrium phonons escape time  $\tau_{\text{esc}}$ . Currently, gain bandwidth of phonon-cooled NbN HEB mixers at the optimal operating point which yields the lowest noise temperature has achieved values of 3.6 GHz for the device on quartz substrate with MgO buffer layer [7], 4 GHz for Si [8], 3.7 GHz for sapphire [8], 4.5 GHz for MgO [2]. Further improvement of NbN phonon-cooled HEB mixers can be achieved through decreasing of  $\tau_{\text{esc}}$ . Phonons escape time depends on film thickness and acoustic transparency of substrate-superconductor interface. In this work we studied the influence of MgO buffer layer on superconducting properties of NbN films of varied thickness. We also researched into gain bandwidth of the devices based on ultrathin NbN films deposited on MgO substrate and on MgO buffer layer on silicon substrate. A gain bandwidth of 5.2 GHz was obtained for a device fabricated from 2 nm thick NbN film deposited on Si substrate with MgO buffer layer.

### **Device design and fabrication.**

In this work NbN HEB mixers on Si and MgO substrates and Si with MgO buffer layer were studied. MgO buffer layer, 200 nm thick, was deposited by e-beam evaporation from MgO pellet. The substrate temperature during the MgO deposition process was about 400 °C.

Ultrathin NbN films were deposited by reactive dc magnetron sputtering in the Ar + N<sub>2</sub> gas mixture. The maximum values of the critical film parameters ( $T_c$  and  $j_c$ ) were reached at the partial Ar pressure of  $5 \times 10^{-3}$  mbar, the partial N<sub>2</sub> pressure of  $9 \times 10^{-5}$  mbar, the discharge current value of 300 mA, the discharge voltage of 300 V and the substrate temperature 850 °C. The deposition rate was 0.5 nm/s. It was defined as the ratio of the film thickness, measured with a Talystep profilometer-profilograph, and its deposition time. The film thickness varied between 2 and 10 nm according to deposition time. The quasi-optical mixer was made by e-beam lithography and photolithography as illustrated in Fig. 1. For fabrication of the devices the central part of spiral antenna was formed using lift-off e-beam lithography based on Cr-Au metallization (Cr ~ 5 nm, Au ~ 70 nm). The gap between the gold contact pads that uncovered the active NbN film area in the mixer was 0.15 – 0.25  $\mu\text{m}$  long and 1.5 – 2.5  $\mu\text{m}$  wide. A SEM photograph of the central part for

one of the devices is presented in Fig. 2b. The next process was to fabricate the outer part of the mixer by lift-off photolithography based on Ti-Au metallization (Ti ~ 5 nm, Au ~ 200 nm) as presented in Fig. 2a. The last process was to remove the NbN layer by ion-milling in Ar atmosphere from the whole substrate surface except for the central part of the spiral antenna, which was protected by a SiO mask made by lift-off e-beam lithography.

An improvement of superconducting properties of NbN ultrathin films due to the presence of MgO buffer layer on silicon substrates is evident and reproducible. As can be seen from Fig. 3, NbN ultrathin films (even those 2 nm thick) deposited on MgO buffer layer have a higher  $T_c$  not only in comparison with NbN films deposited on silicon substrate but also with NbN films deposited on MgO substrate. We believe that this effect can be explained by the fact that surface properties of MgO buffer layers deposited on silicon substrate are better than those of MgO substrate itself. Silicon substrates can be polished more accurately than MgO ones but the discrepancy in thermal coefficient of expansion between silicon and NbN cause high mechanical stresses in the films, which explains worse superconducting properties of the NbN ultrathin films deposited on silicon.

### **Experimental Setup.**

The HEB mixer output power versus intermediate frequency was measured at LO frequency in the range of 0.87-1 THz. The Experimental setup is presented in Fig. 4.

Two backward wave oscillators OB-44 were used as heterodyne and signal sources. Radio frequency (rf) radiation was focused using two Teflon lenses to create optimum patterns. After the attenuation by polarizers rf power was split by 50- $\mu$ m Maylar beam-splitter and arrived into liquid-helium cooled vacuum cryostat through a Teflon window. After IR Zitex filter it fell on mixer block mounted on the cold plate of the cryostat. The mixer block consisted of a hyper-hemispherical lens fabricated from high-resistivity silicon with a mixing device positioned on the flat side of the lens. The device antenna was integrated with 50 Ohm coplanar line. The intermediate frequency signal was guided out of the HEB via a 50 Ohm microstrip line, which was soldered to an SMA connector. A bias tee was used to feed the bias to the mixer and to transmit the intermediate frequency signal to a room temperature amplifier. Because of a limited dynamic range of NbN HEB mixer and a comparably high noise temperature of ultra-wideband amplifiers we used two amplifying chains in the frequency range of 0.5–9 GHz (0.5-4 GHz 55 dB amplifying chain and 3.7-9 GHz 57 dB amplifying chain). The amplified signal power was recorded

by a power meter. The intermediate frequency was measured by a spectrum analyzer connected in a chain after the directional coupler.

When the output power was measured at low signal power versus intermediate frequency we had to use an amplifying chain that consisted of three amplifiers (about 65-80 dB in all frequency ranges). To prevent the noise power of the first amplifier after amplification from coming out of the dynamic range of the last amplifier, a tunable filter was inserted before the last amplifier. The filter had 20 MHz bandpass and the central frequency tuned in the range from 1.8 GHz to 12 GHz. Low input signal power measurements showed that output power about 65 dBm is within the dynamic range of the HEB mixer based on the ultrathin NbN film down to 2 nm thick.

### **Results and Discussion.**

The output power vs. IF dependence was measured under varied operating conditions. The family of IV-curves for one of the devices is presented in Fig. 5. Operating point 1 yields an optimum noise performance of the device and is marked in the figure. Operating point 2 corresponds to the same LO power as operating point 1 and to a higher bias voltage. Measured output power vs. IF dependence of the device in the operating point 1 is presented in Fig. 6 by curve A. Curve B in Fig. 6 presents the measured IF dependence at operating point 2 of the same device. Operating at larger biases than the optimum can decrease a self-heating effect (positive electro-thermal feedback) and therefore expands the gain bandwidth. This can be described by the following equation [9]:

$$\Delta B = \Delta B_0(1+C(R-R_L)/(R+R_L)),$$

where  $R$  is the DC resistance of the sample at the operating point,  $R_L$  is the load resistance of the IF chain, and  $C$  is a self-heating parameter determined by the following equation:

$$C = (I^2(\partial R/\partial T)/c_e V)\tau_0,$$

where  $I$  is the bias current,  $\partial R/\partial T$  is the superconducting transition derivative of the resistance with respect to temperature,  $c_e$  is electron specific heat and  $V$  is active NbN film volume.

The experimental error of the obtained dependencies of the output power vs. intermediate frequency is not small enough due to residue resonances in the IF chain. To reduce this experimental error the output power ratio at two different operating points at each intermediate frequency was analyzed. This ratio IF dependence is presented in Fig. 6 by curve C. It is evident that residue resonance influence is decreased on the ratio curve.

This curve has two characteristic frequencies, corresponding to gain bandwidths of the device at two operating points.

Experimental results for devices based on 3.5 nm thick NbN film on MgO substrate and on MgO buffer layer on silicon substrate are presented in Fig. 7. The cut-off frequency for a device on MgO substrate is in good agreement with an independently obtained value [2]. As can be seen from the figure, the measured values of gain bandwidth for the devices investigated in this work and based on 3.5 nm NbN film are close to each other. The cut-off frequency for a phonon-cooled NbN HEB mixer is determined by electron-phonon interaction time  $\tau_{\text{eph}}$  and non-equilibrium phonons escape time  $\tau_{\text{esc}}$ . It is known from other papers [10] that the gain bandwidth of a device based on 3.5 nm thick NbN film partly depends on  $\tau_{\text{esc}}$  that is determined by film thickness  $d$  and acoustic transparency between active superconducting film and substrate  $\alpha$  as follows:

$$\tau_{\text{esc}} = 4d/\alpha u,$$

where  $u$  is the speed of sound in NbN. According to the result of Fig. 7,  $\alpha$  can be assumed to be the same for MgO substrate and MgO buffer layer on Si substrate because in both cases all other parameters are the same. Consequently, the current MgO buffer layer on silicon substrate has good acoustic transparency to NbN ultrathin film (the same as has the MgO substrate itself) and better surface properties than other investigated substrates.

The noise bandwidth of a device based on 3.5 nm thick NbN film deposited on MgO buffer layer on Si was measured at LO frequency 0.6 THz in the Chalmers University of Technology. The obtained noise temperature vs. IF dependence is presented in Fig. 8. The Intermediate frequency with a noise temperature twice as high as the minimal value was about 5.5 GHz. This is in good agreement with gain bandwidth measurements.

The output power vs. IF dependence for a device based on 2 nm thick NbN film as obtained in this work is presented in Fig. 9. As can be seen from this figure, the gain bandwidth under optimal operation conditions achieved 5.2 GHz, while at higher bias voltage it reached 10.7 GHz. This latter value is in good accordance with the material limit provided by electron-phonon interaction time. This time  $\tau_{\text{eph}}$  for NbN depends on temperature as follows [11]:

$$\tau_{\text{eph}} = 500 \cdot T^{-1.6}$$

The highest  $T_c$  of the devices based on 2 nm thick NbN ultrathin film achieves 9.2 K. According to the equation above,  $\tau_{\text{eph}}$  is about 14.4 ps and provides an overall gain

bandwidth of 11.1 GHz. So, we can presume that in the case of NbN films 2 nm thick HEB mixer's cut-off intermediate frequency mostly depends on  $\tau_{\text{eph}}$  and in its turn on the superconducting transition temperature.

### **References**

1. C.-Y. Edward Tong, Jonathan Kawamura, Todd R. Hunter, D. Cosmo Papa, Raymond Blundell, Michael Smith, Ferdinand Patt, Gregory Goltsman and Eugene Gershenson "Successful operation of a 1 THz NbN hot-electron bolometer receiver", In 11<sup>th</sup> Intl. Sym. On Space Terahertz Technology, pp. 49-59, Ann Arbor, MI (USA), May 2000.
2. M. Kroug, S. Cherednichenko, M. Choumas, H. Merkel, E. Kollberg, H.-W. Huebers, H. Richter, D. Loudkov, B. Voronov, G. Gol'tsman "HEB Quasi-optical Heterodyne Receiver for THz Frequencies", In 12<sup>th</sup> Intl. Sym. On Space Terahertz Technology, pp. 244-252, San Diego, California (USA), 2001.
3. E. M. Gershenson, G. N. Goltsman, I. G. Gogidze, Yu. P. Gousev, A. I. Elantiev, B. S. Karasik, A. D. Semenov "Millimeter and sub-millimeter range mixer based on electronic heating of superconducting film in the resistive state" Sov. Phys. Superconductivity **3**, p. 1582 (1990).
4. D. E. Prober "Superconducting terahertz mixer using a transition-edge microbolometer" Appl. Phys. Lett. **62**, pp. 2119-2121 (1993).
5. R. Wyss, B. Karasik, W. McGrath, B. Bumble and H. LeDuc "Resistive behavior of Nb Diffusion-cooled Nb Hot-Electron Bolometers". In 10<sup>th</sup> Intl. Sym. On Space Terahertz Technology, pp. 215-228, Charlottesville (USA), March 1999.
6. E.M. Gershenson, M.E. Gershenson, G.N. Gol'tsman, A.M. Lyul'kin, and A.D. Semenov. "Electron-phonon interaction in ultrathin Nb films". Sov. Phys. JETP, 70(3): 505-511, March 1990.
7. D. Meledin, C.E. Tong, R. Blundell, N. Kaurova, K.Smirnov, B.Voronov, G. Golt'sman. "Sensitivity and IF bandwidth of waveguide NbN phonon-cooled HEB mixers based on crystalline quartz substrate with MgO buffer layer." this conference proceedings.
8. S. Cherednichenko, P. Yagoubov, K. Il'in, G. Gol'tsman and E. Gershenson "Large Bandwidth of NbN Phonon-Cooled Hot-Electron Bolometer Mixer on Sapphire Substrates" In 8<sup>th</sup> Intl. Sym. On Space Terahertz Technology, pp. 245-252, Cambridge, MA, 1997.
9. E.M. Gershenson, G.N. Gol'tsman, A.I. Elant'ev, B.S. Karasik and S.E. Potoskuev "Intense Electromagnetic Radiation Heating of Electrons of a Superconductor in the resistive state" Sov. J. Temp. Phys.,14(7), 414-420, 1988.
10. S. Cherednichenko, M. Kroug, P. Yagoubov, H. Merkel, E. Kollberg, K. S. Yngvesson, B. Voronov, G. Gol'tsman "IF bandwidth of phonon-cooled HEB mixers made from NbN films

on MgO substrates”, In 11<sup>th</sup> Intl. Sym. On Space Terahertz Technology, pp. 49-59, Ann Arbor, MI (USA), May 2000.

11. G. N. Gol'tsman, A. D. Semenov, Y. P. Gousev, M. A. Zorin, I. G. Gogidze, E. M. Gershenson, P. T. Lang, W. J. Knott and K. F. Renk “Sensitive picosecond NbN detector for radiation from millimeter wavelength to visible light”, Supercond.: Sci. and Technol., vol. 4, 1991, pp. 453-456.

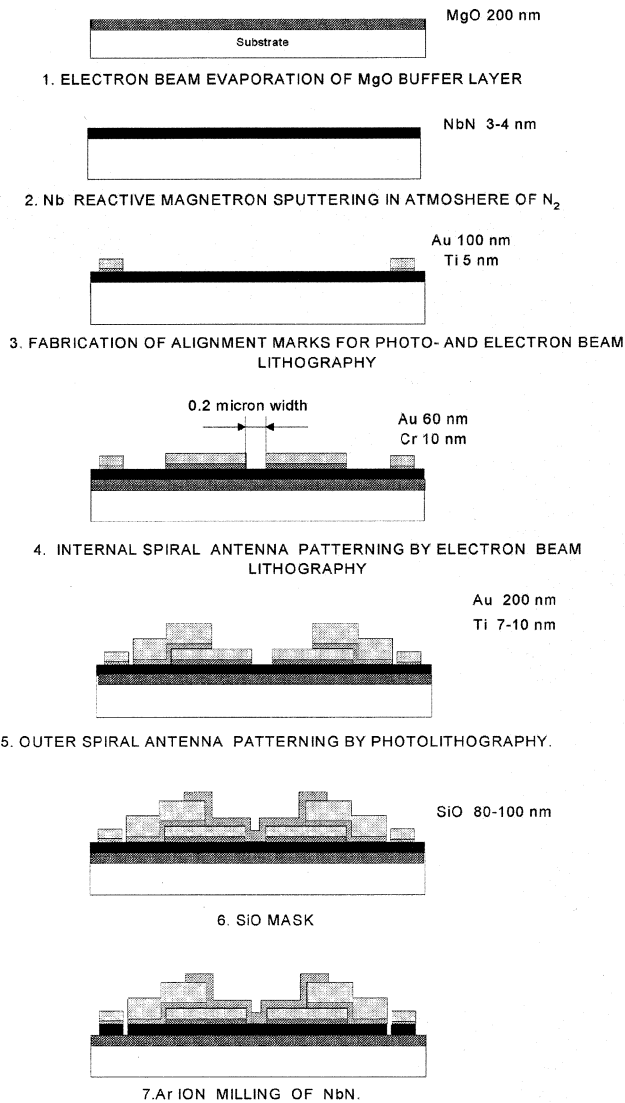


Fig. 1 Fabrication steps for NbN Hot-Electron Bolometer Mixer with MgO Buffer Layer

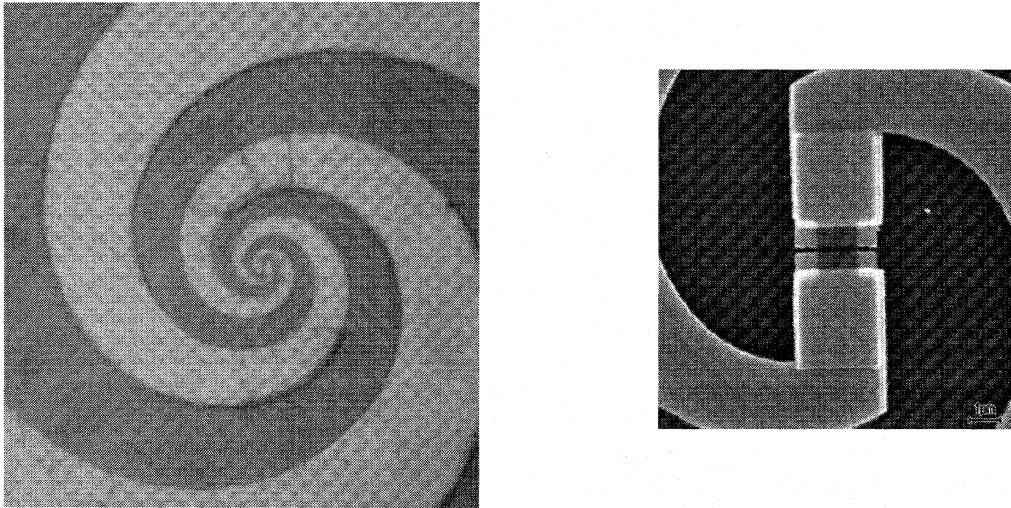


Fig. 2 Photograph of the spiral antenna integrated with the device (Left).  
SEM photo of the central part of the antenna, showing the HEB device (Right)

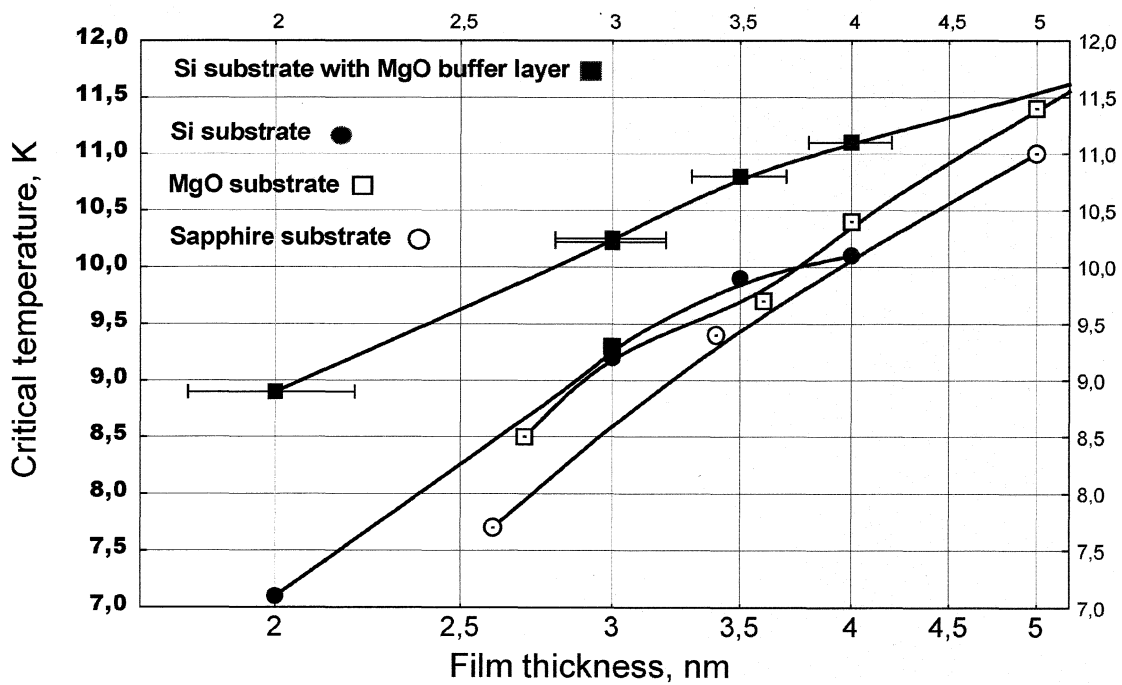


Fig. 3. Critical temperature vs. film thickness for NbN films on different substrates.



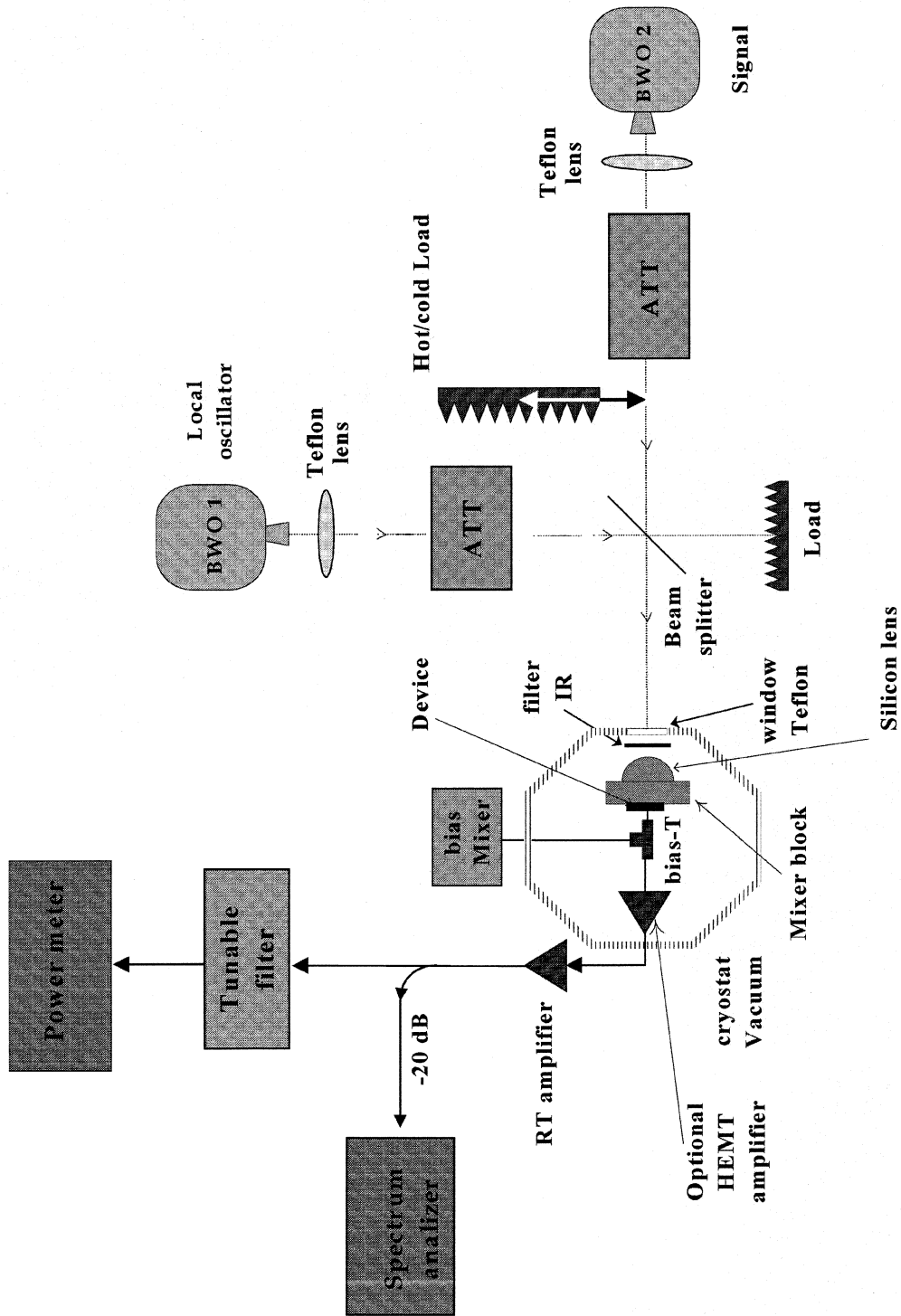


Fig. 4 Experimental setup

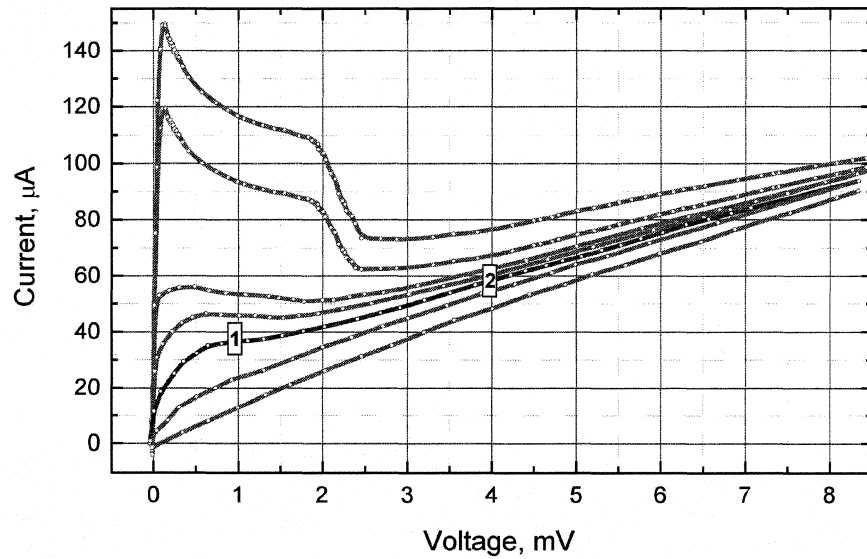


Fig 5. IV curves of device based on 3.5 nm thick NbN film on MgO buffer layer on Si substrate.

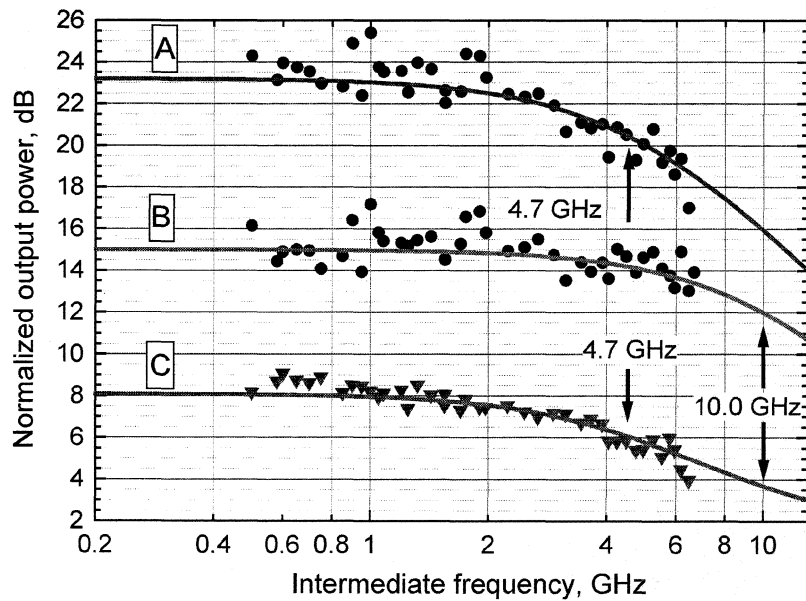


Fig. 6. Output power vs. intermediate frequency at two operating points mentioned on fig. 5 (curves A and B). Curve C presents output power ratio at each intermediate frequency

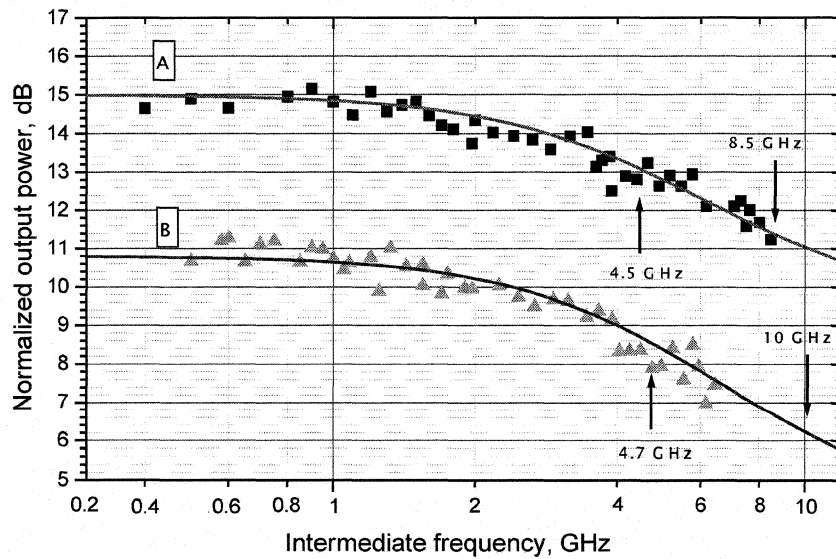


Fig. 7 Output power vs. intermediate frequency dependences for the devices based on 3.5 nm thick NbN film deposited on MgO substrate (A) and Si substrate with MgO buffer layer (B).

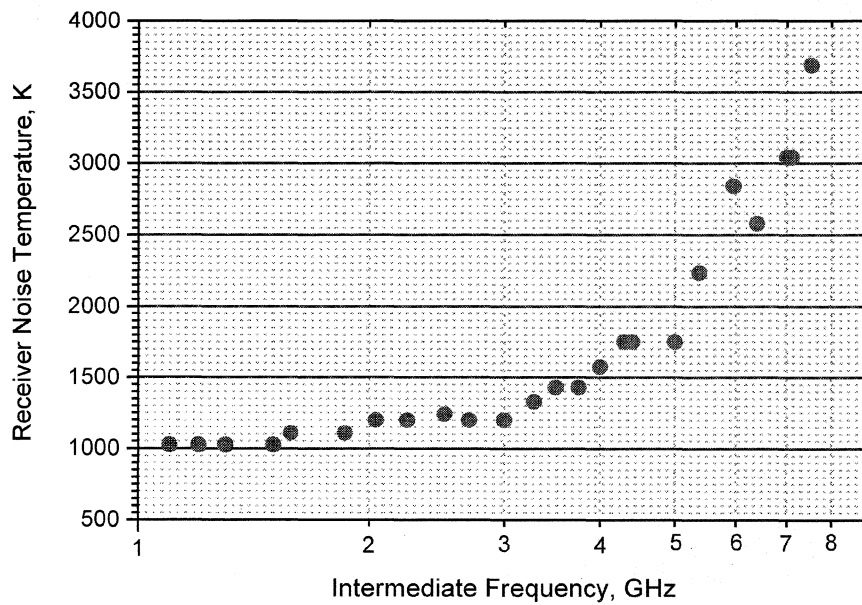


Fig. 8 Noise temperature vs. IF of a device based on 3.5 nm thick NbN film on MgO buffer layer on Si at 0.6 THz LO frequency.

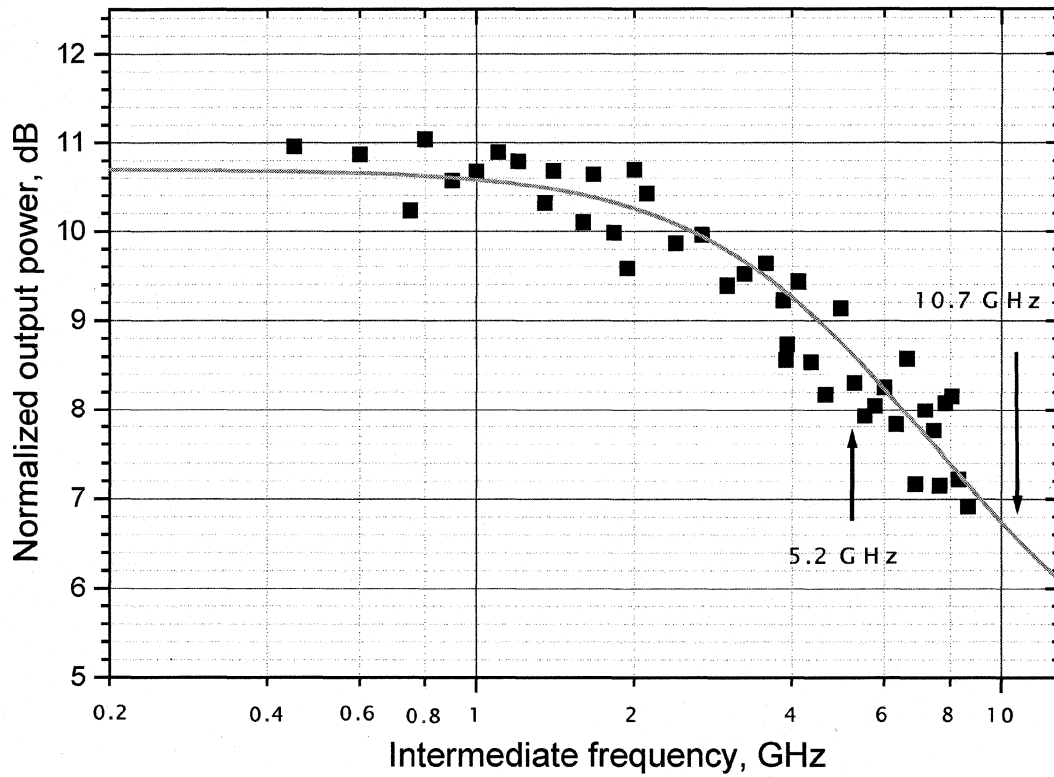


Fig. 9 Output power vs. intermediate frequency dependence for the device based on 2 nm thick NbN film deposited on Si substrate with MgO buffer layer.